

PERSPECTIVE OPEN

Magnetic chirality



Sang-Wook Cheong¹✉ and Xianghan Xu¹

Chirality with all broken mirror symmetries matters ubiquitously from DNA functionality, vine climbing, to the piezoelectricity of quartz crystals. Magnetic chirality means chirality in spin-ordered states or (atomic-scale or mesoscopic) spin textures. Magnetic chirality does not change with time-reversal operation, and chirality prime (C') means that time-reversal symmetry in addition to all mirror symmetries is broken with free spatial rotations. We will discuss a few examples of magnetic chirality and C' , and their emergent physical properties. Some of these exotic properties have been recently observed, and many of them need to be experimentally confirmed.

npj Quantum Materials (2022)7:40; <https://doi.org/10.1038/s41535-022-00447-5>

INTRODUCTION

Chirality refers to the situation where an object and its mirror image cannot overlap to each other by spatial rotation and translation, i.e., all mirror symmetries are broken (or absent) in the object even if any spatial rotation and translation are freely allowed. Our hands are one of the most recognized examples of chirality: the left hand is a nonsuperimposable mirror image of the right hand, even if any spatial rotation and translation are freely allowed. In addition, chirality in steady states has preserved time-reversal symmetry; in other words, left-type chiral objects remain to be left-type under time-reversal symmetry operation. Magnetic chirality means chirality in spin-ordered states or (atomic-scale or mesoscopic) spin textures. Often, magnetic chirality occurs in centrosymmetric magnetic sublattices while their crystallographic lattices are chiral, but not always. For example, helical spin states in rare-earth metals, YMn_6Sn_6 , GdRu_2Si_2 , or $\text{Gd}_3\text{Ru}_4\text{Al}_{12}$ with centrosymmetric crystallographic lattices have magnetic chirality^{1–4}. Examples of “magnetic chirality occurs in centrosymmetric magnetic sublattices while their crystallographic lattices are chiral” include Fe langasite ($\text{Ba}_3\text{NbFe}_3\text{Si}_2\text{O}_{14}$)⁵, $\text{Cr}_{1/3}\text{TaS}_2$ ⁶, and Co-/Mn-doped Ni_3TeO_6 ^{7,8}. Examples of “magnetic chirality occurs in chiral magnetic sublattices when their crystallographic lattices are also chiral” include helical spin states or skyrmion states in B20-structure compounds such as MnSi ⁹. Emphasize that magnetic chirality does not change under time reversal. We call chirality prime (chirality' or C') when all of mirror and time-reversal symmetries are broken even if any spatial rotation is freely allowed. It turns out that C' does exhibit diagonal linear magnetoelectricity¹⁰. Note that in this perspective, we use the notations and concepts in ref. ¹⁰— C : chirality, \mathcal{P} : polarization, a : axially (ferro-rotation), C' : chirality prime, \mathcal{P}' : polarization prime (linear momentum or magnetic toroidal moment), and a' : axially prime (magnetization).

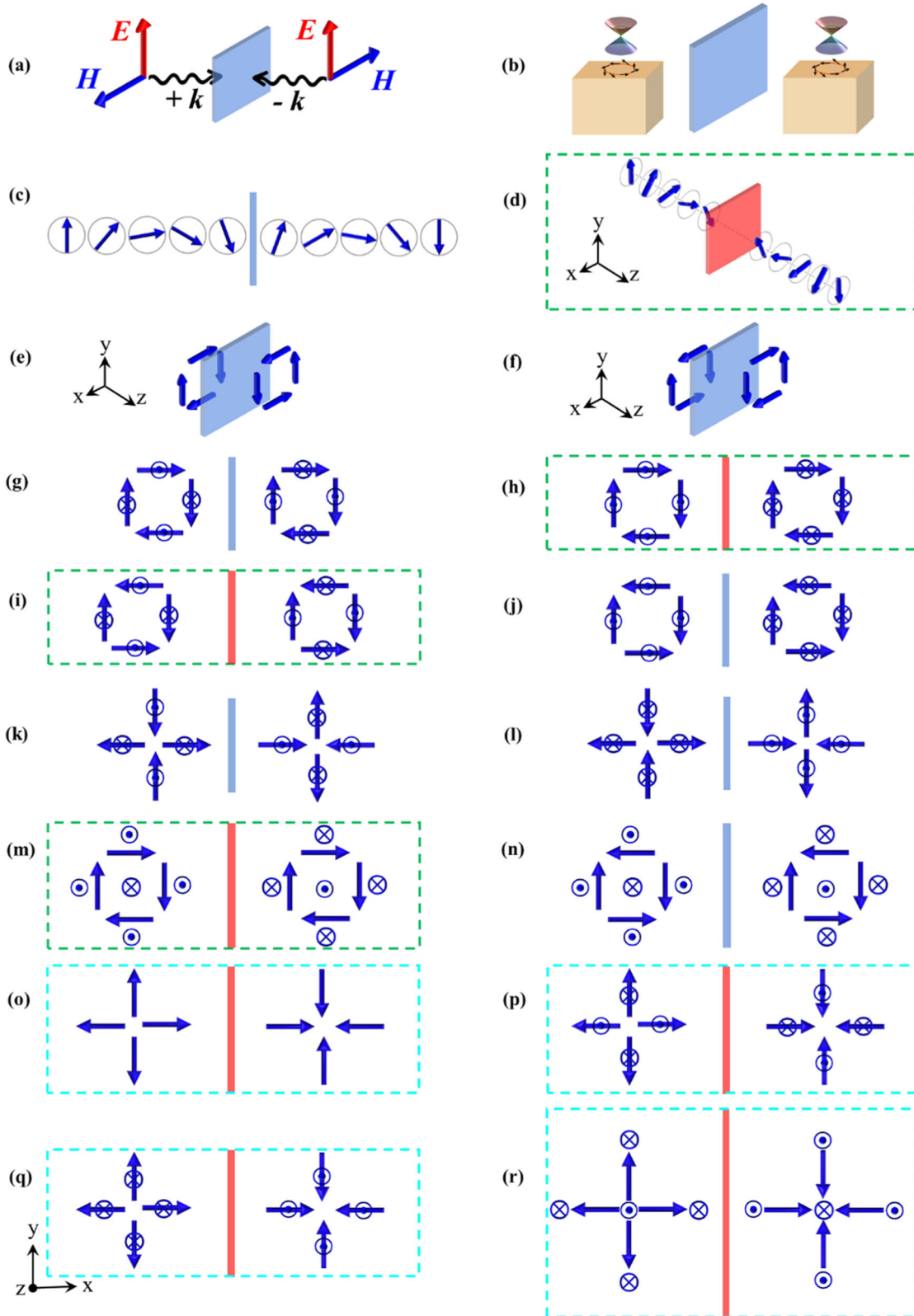
Three exemplary spin textures with magnetic chirality, represented as C , are helical spin order, “toroidal moment + a canted moment”, and “magnetic quadrupole moment + alternating canted moments”¹⁰. Note that Bloch-type ferromagnetic walls are chiral, but Neel-type ferromagnetic walls are achiral. Chirality of “toroidal moment + a canted moment” and that of “magnetic quadrupole moment + alternating canted moments” were first discussed in Ref. ¹⁰, and “toroidal moment + a canted moment” was experimentally discovered in BaCoSiO_4 (magnetic point group

of 6)¹¹, and “magnetic quadrupole moment + alternating canted moments” was experimentally observed in $\text{Pb}(\text{TiO})\text{Cu}_4(\text{PO}_4)_4$ and $\text{Er}_2\text{Ge}_2\text{O}_7$ ^{12,13}. It turns out that circularly polarized light (including X-ray) and vortex beams are, in fact, chiral (i.e., all mirror symmetries with a combination of any spatial rotation are broken—see below for comparison with linearly polarized light), so they can couple with this magnetic chirality as well as crystallographic chirality. Thus, any magnetic chiral systems should have magnetic version of natural optical activity, circular dichroism, etc. This was first proposed in ref. ¹⁴, and in fact, a natural optical activity in a THz range has recently been observed in the helical spin state of CuO with an achiral crystallographic structure¹⁵. In addition, vortex beams, lights with orbital angular momenta, should couple with either crystallographic chirality or magnetic chirality, but these effects have never been studied. In addition, both crystallographic chirality and magnetic chirality can exhibit magnetochiral effects, i.e., directional nonreciprocal effects along the magnetic-field directions in the presence of external magnetic fields. Directional nonreciprocal spin waves in magnets with helical spins (e.g., Er metal with centrosymmetric crystallographic lattice) have been studied¹⁶, but no study of directional nonreciprocal spin waves in “toroidal moment + a canted moment” or “magnetic quadrupole moment + alternating canted moments” has been reported.

CHIRALITY OF PHYSICAL OBJECTS, INCLUDING SPIN TEXTURES

We examine the chirality of many physical objects, including spin textures, in terms of broken or unbroken mirror and time-reversal symmetries in Fig. 1. Note that the spatial rotation is freely allowed in all of the following discussions, e.g., a toroidal moment flips under time reversal, but it can overlap itself by 180° rotation, so we say that the toroidal spin order does not break time-reversal symmetry in this perspective. (a) shows that linearly polarized light is achiral since the mirror is not broken, but circularly polarized light or vortex beams are chiral. We note that the standard spin wave in a ferromagnet and also phonon that can induce a magnetization along a direction perpendicular to the phonon propagation has the symmetry of linearly polarized light, so they are achiral, even though the terms of chiral phonon and chiral magnon have been sometimes used mistakenly^{17,18}. (b) shows that the surface state of topological insulators is achiral (in fact, no reason why it can be chiral since there is no structural chirality and

¹Rutgers Center for Emergent Materials and Department of Physics and Astronomy, Rutgers University, New Jersey, USA. ✉email: sangc@physics.rutgers.edu



also no frustrated interactions that can lead to magnetic chirality there), even though the terms of chiral surface states or chiral edge states are often used for topological materials incorrectly¹⁹. (c) and (d) display cycloidal and helical spins, respectively. The cycloidal spin order has a mirror symmetry perpendicular to the

propagation direction, therefore it is achiral, and has symmetry operational similarity (SOS) with a polarization parallel to the mirror plane¹⁴. The SOS means that an object has equal or lower, but not higher symmetries, compared with a measurable such as polarization. The helical spin order breaks all mirror symmetries.

Fig. 1 Various spin textures and their symmetry properties. Blue and red arrows show spins and electric fields, respectively. Blue (red) mirrors mean that the original and its mirror images can (cannot) overlap by spatial rotation. For each object in cyan boxes (o–r), the original and its time reversal images cannot overlap by spatial rotation, so **T** is broken. **T** is not broken for the rest cases. Dashed green box means chiral C , i.e., magnetically chiral (broken mirrors, and unbroken **T**). Dashed cyan box means chirality prime C' , i.e., diagonal linear magnetoelectric (both mirror and **T** broken). **a** Linearly polarized light. **b** The topological surface state of topological insulator. **c** Cycloidal spins, Neel-type ferromagnetic walls. **d** Helical spins, Bloch-type ferromagnetic walls. **e** Magnetic toroidal moment or magnetic vortex. **f** Type-I magnetic quadrupole or magnetic anti-vortex. **g** Magnetic toroidal moment or magnetic vortex with alternating canted moments. **h** Magnetic toroidal moment or magnetic vortex with a canted moment. **i** Type-I magnetic quadrupole with alternating canted moments. **j** Type-I magnetic quadrupole with a canted moment. **k** Type-II magnetic quadrupole with alternating canted moments. **l** Type-II magnetic quadrupole with a canted moment. **m** Bloch-type skyrmion. **n** Anti-skyrmion. **o** Magnetic monopole. **p** Magnetic monopole with alternating canted moments. **q** Magnetic monopole with a canted moment **r** Neel-type skyrmion.

Meanwhile, it does not break time reversal. So, helical spin order does show magnetic chirality. (e) and (f) show that a toroidal spin order and type-I magnetic quadrupole without any canted moment have mirror planes parallel to all spins, so they are achiral. (g) and (j) show that toroidal spin order with alternating canted moments and type-I magnetic quadrupole with a canted moment still have mirror symmetry perpendicular to the screen, so they are still achiral. (h) A toroidal spin order with a canted moment breaks all mirror symmetries, but does not break time reversal. Therefore, it holds magnetic chirality, and has been observed in BaCoSiO_4 ¹¹. Type-I magnetic quadrupole with alternating canted moments shown in (i) also holds magnetic chirality. (k) and (l) represent type-II magnetic quadrupoles with alternating canted moments and that with a canted moment, respectively, and none of them are chiral. (m) shows that a Bloch-type skyrmion has magnetic chirality, while an antiskyrmion shown in (n) has mirror symmetry perpendicular to the screen, so it is achiral. (o), (p), (q), and (r) represent magnetic monopole, magnetic monopole with alternating canted moments, magnetic monopole with a canted moment, and Neel-type skyrmion, respectively. None of them have mirror symmetries, however, they are not chiral since they all have broken time reversal. Instead, they are chiral' (C'). This discussion brings up a number of important observations. It turns out that Bloch-type skyrmions have magnetic chirality, even though Neel-type skyrmions are achiral. Thus, Bloch-type skyrmions in magnetic fields can exhibit directional nonreciprocity, which has been reported^{20–22}. Anti-skyrmions are neither C nor C' , which is consistent with the fact that anti-skyrmions are not observed in structurally chiral materials. Moreover, it turns out that among all canted-moment or alternating-canted-moment type-I or -II magnetic quadrupoles, only type-I magnetic quadrupole with alternating canted moments is chiral. Materials with magnetic quadrupoles include $\text{Pb}(\text{TiO})\text{Cu}_4(\text{PO}_4)_4$ and $\text{Er}_2\text{Ge}_2\text{O}_7$ ^{12,13}. They both have chiral crystallographic structures and complicated magnetic sublattices. It turns out that their complex magnetic structures can be treated as a combination of type-I and -II quadrupoles, both with alternating canted moments, and the intriguing magnetoelectric properties of $\text{Pb}(\text{TiO})\text{Cu}_4(\text{PO}_4)_4$ can be neatly explained by the magnetic chirality of the type-I quadrupole with alternating canted moments (see below). Notably, the chirality from alternating-canted-moment type-I quadrupoles is invariant among different clusters within one unit cell, which guarantees the single magnetic chirality of the whole spin state, fixed by the overall crystallographic chirality. Note that the relevant magnetoelectric properties of $\text{Er}_2\text{Ge}_2\text{O}_7$ have not been reported yet. These two examples demonstrate that the symmetry-analysis strategy in the present perspective can be successfully applied to even extremely complicated magnetic states.

MATERIALS WITH CHIRALITY

A structural chirality may lead to a magnetic chirality. Some reported magnetic compounds with chiral crystallographic lattices are reviewed. Fe langasite ($\text{Ba}_3\text{NbFe}_3\text{Si}_2\text{O}_{14}$) forms in a

chiral crystallographic lattice with centrosymmetric magnetic sublattice, and its magnetic ground state is a helical spin order⁵. Its magnetochiral effect, i.e., directional nonreciprocal spin-wave propagation in magnetic fields, has been observed²³. $\text{RENi}_3(\text{Al}, \text{Ga})_9$ (RE = rare earths) has chiral crystallographic lattice and centrosymmetric magnetic sublattice²⁴. Although it is a candidate for magnetic chirality, the magnetic structure is not clear yet²⁵. Some compounds with B20 structure such as $\text{Co}_7\text{Zn}_7\text{Mn}_6$ ²⁶, MnSi_9 , MnGe_7 ²⁷, $\text{Fe}_{1-x}\text{Co}_x\text{Si}_2$ ²⁸, and Cu_2OSeO_3 ²⁹ have chiral crystallographic lattices, chiral magnetic lattices, helical spin-ground states, and Bloch-type skyrmion state in magnetic fields. Interestingly, it was reported that the helical magnetic chirality can change for a fixed crystallographic chirality when the Dzyaloshinskii–Moriya (DM) interaction sign changes by doping in $\text{Co}_{8-x}\text{Fe}_x\text{Zn}_8\text{Mn}_4$, $\text{Mn}_{1-x}\text{Fe}_x\text{Ge}$, and $\text{Fe}_{1-x}\text{Co}_x\text{Ge}$ ^{30–33}. Directional nonreciprocity has been observed in the helical spin and Bloch-type skyrmion states of MnSi and CuOSeO_3 ^{20–22}. In the hexaoxotellurate family having chiral and polar crystallographic lattice (space group $R3$), Ni_3TeO_6 has a collinear antiferromagnetic ground state³⁴, which is achiral. However, the high-field magnetic state does exhibit magnetic chirality³⁵. With Mn/Co doping, incommensurate helical magnetism occurs with magnetic chirality^{7,8}. $\text{Ni}_2\text{InSbO}_6$ holds a cycloidal spin order³⁶, which is achiral. The crystallographic space groups, magnetic point groups, chirality of magnetic sublattice, and the type of spin texture of some of these compounds are summarized in Supplementary Table 1.

ROTATIONAL PROPERTIES OF MAGNETIC CHIRALITY

Now, we discuss the spatial rotational properties of magnetic chiral objects. Each of all four magnetic chiral objects that we have discussed above has one well-defined direction (the z direction in Fig. 1), along which a high rotational symmetry such as C_4 or C_2 exists, and this direction is called chiral axis for the sake of convenience (chiral axis does not mean that it is chiral). Now, 2-fold rotational property along an axis in the plane perpendicular to the chiral axis, varies: helical spin state has C_2 along x or y , “toroidal moment + a canted moment” has broken C_2 along x or y , “Type-I magnetic quadrupole moment + alternating canted moments” has broken C_2 along x or y , but unbroken C_2 along xy or yx , and a Bloch-type skyrmion has broken C_2 along x or y . Optical activities with circularly polarized light or vortex beams require broken $\{\mathbf{M}, \mathbf{M} \otimes \mathbf{R}, \mathbf{I} \otimes \mathbf{T}\}$ (note that the symbol \otimes means a combination of two consecutive symmetry operations, see Ref. 14 for definitions of others), so among 1D objects, they can couple with C and C' ¹⁰. Therefore, magnetic chirality can exhibit optical activities. However, if magnetic chirality is fixed by crystallographic chirality, then inverse Faraday effect cannot induce flipping between two types of magnetic chiral domains. Thus, flipping between two types of magnetic chiral domains through inverse Faraday effect with circularly polarized light or vortex beams can occur in magnetic chiral systems on centrosymmetric crystallographic lattice such as rare-earth metals or YMn_6Sn_6 with helical spin order or Gd_2PdSi_3 (centrosymmetric $P6/mmm$ lattice) with

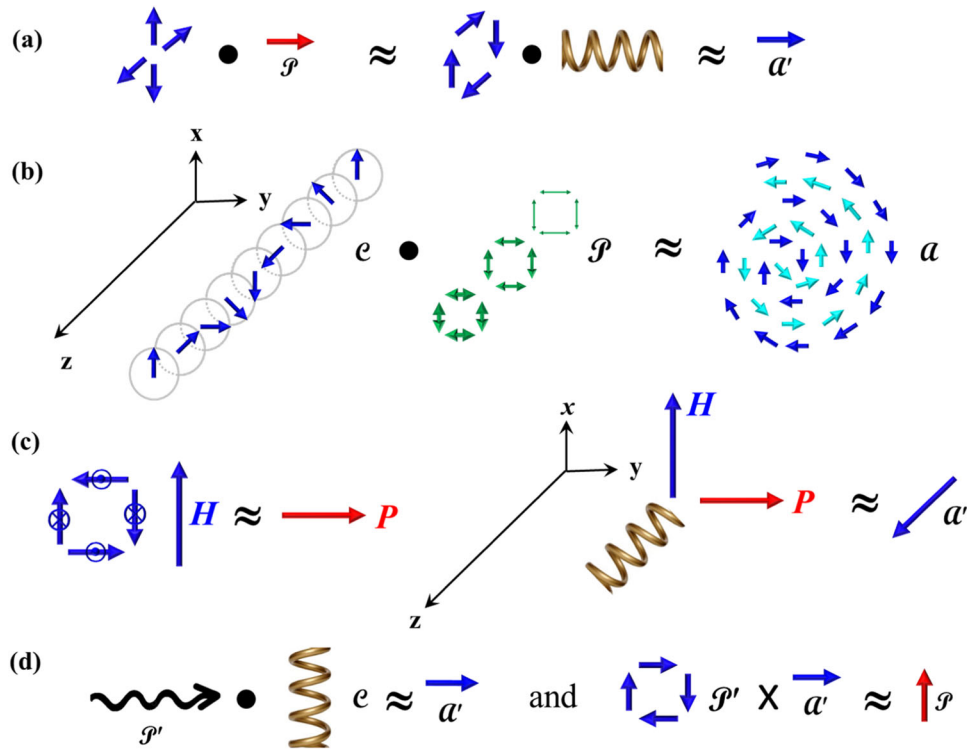


Fig. 2 Emergent phenomena of various objects, mostly spin textures, in the presence of external perturbations. Green double arrows with different thickness show a strain gradient. Other symbols have the same meaning as Fig. 1. **a** Magnetic monopole combined with polarization and toroidal moment combined with crystallographic chirality result in magnetization. **b** Helical spin order in the xy plane under strain gradient along z results in spiral magnetic superstructure. Blue and cyan arrows display spins with different directions. **c** The left cartoon shows how polarization (\mathbf{P}) can be induced in “Type-I magnetic quadrupole + alternating canted moments” by magnetic field (\mathbf{H}). These \mathbf{P} and \mathbf{H} result in a toroidal moment along z , and crystallographic chirality combined with this toroidal moment results in magnetization along z , as shown in the right cartoon. **d** Electric current flow to chirality (crystallographic or magnetic chirality) produces magnetic field along the current direction, and this magnetic field acting on the magnetic toroidal moments of skyrmions or “toroidal moment + a canted moment” results in voltage gradient along the transverse direction, which is the origin of the so-called topological anomalous Hall effect in conducting specimens. In addition, the right-hand-side SOS relationship leads to the off-diagonal linear magnetoelectricity of toroidal moment in insulating specimens.

helical spin order or magnetic bubbles in magnetic fields³⁷. This control of magnetic chirality with circularly polarized light or vortex beams can be an exciting topic for future research.

EMERGENT PHYSICAL PHENOMENA BY MAGNETIC CHIRALITY

The SOS concept and dot products in ref. 10 are used in the following discussion. A magnetic monopole does not have mirror symmetry; however, it is \mathcal{C}' , not \mathcal{C} , because time reversal is also broken and links mirror-reflected states. Materials having magnetic monopole ground states are very rare, and one example is the A_2 phase in hexagonal $\text{Lu}(\text{Fe},\text{Mn})\text{O}_3$ ³⁸. As shown in Fig. 2a, a magnetic monopole combined with a polarization \mathcal{P} induces a magnetization a' parallel to the polarization, therefore, a magnetic monopole is a diagonal linear magnetoelectric³⁹. In fact, all \mathcal{C}' objects are supposed to be diagonal linear magnetoelectric. Similarly, a magnetic toroidal moment \mathcal{P}' with crystallographic chirality \mathcal{C} results in a magnetization a' too. In this case, the chiral axis is perpendicular to the spin plane and parallel to the induced magnetization. An example is that BaCoSiO_4 shows a canted moment in addition to toroidal moment and chiral crystallographic lattice¹¹. In fact, the “toroidal moment + a canted moment” with magnetic chirality in BaCoSiO_4 appears through this self-consistent manner. A magnetically chiral helical spin order \mathcal{C} with the presence of a strain gradient \mathcal{P} can create a spiral magnetic superstructure with the characteristics of A shown in Fig. 2b, and it has been observed in $\text{Cr}_{1/3}\text{TaS}_2$ ⁴⁰. The rotation direction (i.e., clockwise vs. counterclockwise) of magnetic spiral

superstructure depends on the sign of strain gradient (Supplementary Fig. 1). The left cartoon in Fig. 2c shows how polarization (\mathbf{P}) can be induced in type-I magnetic quadrupole by magnetic field (\mathbf{H}), these \mathbf{P} and \mathbf{H} result in a toroidal moment along z , and crystallographic chirality combined with this toroidal moment results in a magnetization a' along z . These cartoons concisely explain the complicated magnetoelectric behavior in $\text{Pb}(\text{TiO})\text{Cu}_4(\text{PO}_4)_4$ and a similar magnetoelectric behavior is expected in $\text{Er}_2\text{Ge}_2\text{O}_7$ (four different configurations are shown in Supplementary Fig. 2). As shown in Fig. 2d, when a current \mathcal{P}' flowing through crystallographic or magnetic chirality \mathcal{C} , they create magnetization a' . The magnetization can further induce a polarization along the transverse direction through the off-diagonal linear magnetoelectricity of the magnetic toroidal component in Bloch-type skyrmions or “toroidal moment + a canted moment”. This mechanism explains the origin of the so-called topological anomalous Hall effect in conducting specimens⁴¹. Both current and Bloch-type skyrmions (or “toroidal moment + a canted moment”) have broken \mathcal{C}_2 , and flipping either of them would reverse the Hall signal sign (Supplementary Fig. 3). In “toroidal moment + a canted moment” case, the flipping of canted moment and/or current in different chiral domains gives opposite Hall-like signal (Supplementary Fig. 4). In addition, the right-hand-side SOS relationship in Fig. 2d leads to the off-diagonal linear magnetoelectricity of toroidal moment in insulating specimens. Properties such as scalar chirality $= \sum \mathbf{S}_i \cdot (\mathbf{S}_j \times \mathbf{S}_k)$, vector chirality $= \sum \mathbf{S}_i \times \mathbf{S}_j$, and octupolar chirality $= \sum \mathbf{S}_i \times (\mathbf{S}_j \times \mathbf{S}_k) = \sum [\mathbf{S}_j (\mathbf{S}_k \cdot \mathbf{S}_i) - \mathbf{S}_k (\mathbf{S}_i \cdot \mathbf{S}_j)]$ of “toroidal moment + a canted

moment" and "type-I magnetic quadrupole + alternatingly canted moments" are summarized in Supplementary Table 2 and 3, respectively. As shown in Supplementary Table 2, the scalar chirality follows the canted moment in "toroidal moment + a canted moment". Interestingly, the octupolar chirality has a one-to-one correspondence to the AHE signal. Note that the octupolar chirality, however, becomes zero in the case of "toroidal moment + a canted moment" on a triangle, rather than a square. Supplementary Table 3 shows that scalar, vector, and octupolar chiralities are zero in "Type-I magnetic quadrupole + alternating canted moments", and they do not account for the expected AHE signal.

Now, magnetic chirality can be controlled by using the simultaneous presence of current and magnetic field. The simultaneous presence of current and magnetic fields, is, in fact, chiral since all mirror symmetries are broken without time reversal breaking even if any spatial rotations are allowed, so the relative sign of coexisting current and magnetic field favors energetically one chirality versus the other chirality, so that it can control the chirality of, for example, helical spin states⁴². Each of Bloch-type skyrmion or magnetic bubble is chiral since all mirror symmetries are broken without time-reversal breaking even if any spatial rotations are allowed. However, Bloch-type skyrmions have mono chirality and magnetic bubbles have random chirality. However, our prediction is magnetic bubbles with mono chirality can be induced using the simultaneous presence of current and magnetic field along one direction, and the change of the relative sign of coexisting current and magnetic field can induce the chirality flipping. For example, Gd_2PdSi_3 can host magnetic bubbles in magnetic fields, and the magnetic chirality of these bubbles can be manipulated by the simultaneous presence of current and magnetic field^{43,44}.

MAGNETIC POINT GROUPS WITH CHIRALITY OR CHIRALITY PRIME

Finally, we provide general notes on chirality in terms of magnetic point groups. First, note that in the four C' cases in Fig. 10–r having broken \mathbf{T} with free spatial rotations, both \mathbf{T} and \mathbf{I} result in the same state, so $\mathbf{I}\otimes\mathbf{T}$ is unbroken with free spatial rotations – we call this kind as type I C' . We can also have magnetic states with all broken mirrors, \mathbf{T} and $\mathbf{I}\otimes\mathbf{T}$ symmetries with free spatial rotations, are coined as type II C' . Examples include magnetic point groups such as 1, 2, 3, 4, 6, 23, 32, 222, 422, 622, and 432. These type-II C' magnetic point groups, in addition to the C magnetic point groups, are usually considered as a part of chiral point groups, and do have lower symmetries than C and also C' (i.e., SOS with C and also C'), so they exhibit all of diagonal linear magnetoelectricity, optical activity, and directional nonreciprocity along the magnetic field direction in magnetic fields. $\bar{1}$, $\bar{4}$, $\bar{3}m'$, and $m'm'2$ are examples of the type-I C' magnetic point group and the C magnetic point groups include $2'$, $4'$, $6'$, $32'$, $11'$, $21'$, $31'$, $321'$, $231'$, $61'$, $2221'$, $4221'$, $6221'$, $6'22'$, $4321'$, and $4'32'$.

SUMMARY

In summary, magnetic chirality refers to atomic-scale or mesoscopic spin textures with all broken mirror symmetries and preserved time-reversal symmetry, and it provides a great platform to study cross-coupled ferroic orders, magnetic optical activities, and topological transport properties. Four types of magnetic chirality have been identified: (1) helical spin order, (2) "toroidal moment + a canted moment", (3) "Type-I magnetic quadrupole moment + alternating canted moments", and (4) Bloch-type skyrmions. To search for new candidates for magnetic chirality, various ingredients need to be considered: canted spins through the DM interaction are necessary for the type-(2) and type-(3) magnetic chiralities, and magnetic frustration can also

provide opportunities for noncolinear spin orders such as helical spin order, magnetic toroidicity, and magnetic quadrupoles. Numerous new experiments and emergent properties associated with magnetic chirality are proposed/predicted, for example, (a) natural optical activities associated with magnetic chirality need to be further explored, and circular dichroism due to magnetic chirality, especially in the cases without bulk net magnetic moment, needs to be studied, (b) magnetochiral effects (i.e., the directional nonreciprocity in the presence of external magnetic fields) of "toroidal moment + a canted moment" and "Type-I magnetic quadrupole moment + alternating canted moments" need to be investigated, (c) the true magnetic ground state of some compounds with chiral crystallographic lattices, especially triangular lattices, should be carefully re-examined—an example is $\text{RENi}_3(\text{Al,Ga})_9$, (d) magnetoelectric properties of $\text{Er}_2\text{Ge}_2\text{O}_7$ need to be studied, (e) the magnetic chirality of helical spin states in centrosymmetric crystallographic lattices can be controlled by circularly polarized light or vortex beams, (f) how vortex beams with orbital angular momentum can couple with either crystallographic chirality or magnetic chirality can be an exciting future research topic, (g) magnetic bubbles with mono chirality can be induced using the coexisting current and magnetic field along one direction, etc. Note that our discussion has been focused on broken symmetries, and the magnitudes of the resulting effects or coupling strengths cannot be estimated from symmetry consideration without understanding the microscopic mechanism. Anyhow, magnetic chirality is a crisp concept for the exploration of the new emergent physical phenomena in complex magnetic systems.

DATA AVAILABILITY

Data sharing not applicable to this article as no datasets were generated or analyzed during the current study.

Received: 10 November 2021; Accepted: 7 March 2022;

Published online: 08 April 2022

REFERENCES

- Koehler, W. C., Cable, J. W., Wilkinson, M. K. & Wollan, E. O. Magnetic structures of Holmium. I. The virgin state. *Phys. Rev.* **151**, 414–424 (1966).
- Ghimire, N. J. et al. Competing magnetic phases and fluctuation-driven scalar spin chirality in the kagome metal YMn_6Sn_6 . *Sci. Adv.* **6**, eabe2680 (2020).
- Khanh, N. D. et al. Nanometric square skyrmion lattice in a centrosymmetric tetragonal magnet. *Nat. Nanotechnol.* **15**, 444–449 (2020).
- Hirschberger, M. et al. Skyrmion phase and competing magnetic orders on a breathing kagome lattice. *Nat. Commun.* **10**, 5831 (2019).
- Marty, K. et al. Single domain magnetic helicity and triangular chirality in structurally enantiopure $\text{Ba}_3\text{NbFe}_3\text{Si}_2\text{O}^{14}$. *Phys. Rev. Lett.* **101**, 247201 (2008).
- Moriya, T. & Miyadai, T. Evidence for the helical spin structure due to antisymmetric exchange interaction in Cr1/3NbS_2 . *Solid State Commun.* **42**, 209–212 (1982).
- Skiadopoulou, S. et al. Structural, magnetic, and spin dynamical properties of the polar antiferromagnets $\text{Ni}_3\text{-xCoxTeO}_6$ ($x = 1, 2$). *Phys. Rev. B* **101**, 014429 (2020).
- Kim, J. et al. Helical versus collinear antiferromagnetic order tuned by magnetic anisotropy in polar and chiral $(\text{Ni,Mn})_3\text{TeO}_6$. *Phys. Rev. Mater.* **5**, 094405 (2021).
- Nakajima, T. et al. Skyrmion lattice structural transition in MnSi . *Sci. Adv.* **3**, e1602562 (2017).
- Cheong, S.-W., Lim, S., Du, K. & Huang, F.-T. Permutable SOS (symmetry operational similarity). *npj Quantum Mater.* **6**, 58 (2021).
- Ding, L. et al. Field-tunable toroidal moment in a chiral-lattice magnet. *Nat. Commun.* **12**, 5339 (2021).
- Kimura, K., Kato, Y., Kimura, S., Motome, Y. & Kimura, T. Crystal-chirality-dependent control of magnetic domains in a time-reversal-broken antiferromagnet. *npj Quantum Mater.* **6**, 54 (2021).
- Taddei, K. M. et al. Local-Ising-type magnetic order and metamagnetism in the rare-earth pyrogermanate $\text{Er}_2\text{Ge}_2\text{O}_7$. *Phys. Rev. Mater.* **3**, 014405 (2019).
- Cheong, S.-W. SOS: symmetry-operational similarity. *npj Quantum Mater.* **4**, 53 (2019).
- Masuda, R., Kaneko, Y., Tokura, Y. & Takahashi, Y. Electric field control of natural optical activity in a multiferroic helimagnet. *Science* **372**, 496–500 (2021).

16. Nicklow, R. M., Wakabayashi, N., Wilkinson, M. K. & Reed, R. E. Spin-wave dispersion relation for Er metal at 4.5 K. *Phys. Rev. Lett.* **27**, 334–337 (1971).
17. Zhu, H. et al. Observation of chiral phonons. *Science* **359**, 579–582 (2018).
18. Liu, Y. et al. Switching magnon chirality in artificial antiferromagnet. *arXiv preprint arXiv:2103.14483* (2021).
19. Zhang, F., Kane, C. L. & Mele, E. J. Surface state magnetization and chiral edge states on topological insulators. *Phys. Rev. Lett.* **110**, 046404 (2013).
20. Weber, T. et al. Polarized inelastic neutron scattering of nonreciprocal spin waves in MnSi. *Phys. Rev. B* **100**, 060404 (2019).
21. Yokouchi, T. et al. Electrical magnetochiral effect induced by chiral spin fluctuations. *Nat. Commun.* **8**, 866 (2017).
22. Seki, S. et al. Propagation dynamics of spin excitations along skyrmion strings. *Nat. Commun.* **11**, 256 (2020).
23. Stock, C. et al. Spin-wave directional anisotropies in antiferromagnetic Ba₃Nb-Fe₃Si₂O¹⁴. *Phys. Rev. B* **100**, 134429 (2019).
24. Silva, L. S. et al. Crystal field effects in the intermetallic RNi₃Ga₉ (R = Tb, Dy, Ho, and Er) compounds. *Phys. Rev. B* **95**, 134434 (2017).
25. Iba, K. et al. In *Proceedings of the International Conference on Strongly Correlated Electron Systems (SCES2019) 30 JPS Conference Proceedings* (JPS, 2020).
26. Ukleev, V. et al. Frustration-driven magnetic fluctuations as the origin of the low-temperature skyrmion phase in Co₇Zn₇Mn₆. *npj Quantum Mater.* **6**, 40 (2021).
27. Tanigaki, T. et al. Real-space observation of short-period cubic lattice of skyrmions in MnGe. *Nano Lett.* **15**, 5438–5442 (2015).
28. Münzer, W. et al. Skyrmion lattice in the doped semiconductor Fe_{1-x}CoxSi. *Phys. Rev. B* **81**, 041203 (2010).
29. Onose, Y., Okamura, Y., Seki, S., Ishiwata, S. & Tokura, Y. Observation of magnetic excitations of skyrmion crystal in a helimagnetic insulator Cu₂OSeO₃. *Phys. Rev. Lett.* **109**, 037603 (2012).
30. Karube, K. et al. Controlling the helicity of magnetic skyrmions in a β-Mn-type high-temperature chiral magnet. *Phys. Rev.* **B98**, 155120 (2018).
31. Grigoriev, S. V. et al. Chiral properties of structure and magnetism in Mn_{1-x}FexGe compounds: when the left and the right are fighting, who wins? *Phys. Rev. Lett.* **110**, 207201 (2013).
32. Shibata, K. et al. Towards control of the size and helicity of skyrmions in helimagnetic alloys by spin-orbit coupling. *Nat. Nanotechnol.* **8**, 723–728 (2013).
33. Grigoriev, S. V. et al. Flip of spin helix chirality and ferromagnetic state in Fe_{1-x}CoxGe compounds. *Phys. Rev. B* **90**, 174414 (2014).
34. Kim, J. W. et al. Successive magnetic-field-induced transitions and colossal magnetoelectric effect in Ni₃TeO₆. *Phys. Rev. Lett.* **115**, 137201 (2015).
35. Lass, J. et al. Field-induced magnetic incommensurability in multiferroic Ni₃TeO₆. *Phys. Rev. B* **101**, 054415 (2020).
36. Ivanov, S. A. et al. Spin and dipole ordering in Ni₂InSbO₆ and Ni₂ScSbO₆ with corundum-related structure. *Chem. Mater.* **25**, 935–945 (2013).
37. Kurumaji, T. et al. Skyrmion lattice with a giant topological Hall effect in a frustrated triangular-lattice magnet. *Science* **365**, 914–918 (2019).
38. Disseler, S. M. et al. Multiferroicity in doped hexagonal LuFeO₃. *Phys. Rev. B* **92**, 054435 (2015).
39. Cheong, S.-W. Trompe L'oeil ferromagnetism. *npj Quantum Mater.* **5**, 37 (2020).
40. Du, K. et al. Topological spin/structure couplings in layered chiral magnet Cr_{1/3}Ta_{5/3}: the discovery of spiral magnetic superstructure. *Proc. Natl Acad. Sci. USA* **118**, e2023337118 (2021).
41. Neubauer, A. et al. Topological Hall effect in the phase of MnSi. *Phys. Rev. Lett.* **102**, 186602 (2009).
42. Jiang, N., Nii, Y., Arisawa, H., Saitoh, E. & Onose, Y. Electric current control of spin helicity in an itinerant helimagnet. *Nat. Commun.* **11**, 1601 (2020).
43. Leonov, A. O. & Mostovoy, M. Multiply periodic states and isolated skyrmions in an anisotropic frustrated magnet. *Nat. Commun.* **6**, 8275 (2015).
44. Okubo, T., Chung, S. & Kawamura, H. Multiple-q States and the skyrmion lattice of the triangular-lattice Heisenberg antiferromagnet under magnetic fields. *Phys. Rev. Lett.* **108**, 017206 (2012).

ACKNOWLEDGEMENTS

The work was supported by the DOE under Grant No. DOE-DE-FG02-07ER46382. We thank Fei-Ting Huang for highly beneficial discussions on the symmetries of magnetic point groups.

AUTHOR CONTRIBUTIONS

S.-W. C. and X.X. wrote the paper.

COMPETING INTERESTS

The authors declare no competing interests.

ADDITIONAL INFORMATION

Supplementary information The online version contains supplementary material available at <https://doi.org/10.1038/s41535-022-00447-5>.

Correspondence and requests for materials should be addressed to Sang-Wook Cheong.

Reprints and permission information is available at <http://www.nature.com/reprints>

Publisher's note Springer Nature remains neutral with regard to jurisdictional claims in published maps and institutional affiliations.



Open Access This article is licensed under a Creative Commons Attribution 4.0 International License, which permits use, sharing, adaptation, distribution and reproduction in any medium or format, as long as you give appropriate credit to the original author(s) and the source, provide a link to the Creative Commons license, and indicate if changes were made. The images or other third party material in this article are included in the article's Creative Commons license, unless indicated otherwise in a credit line to the material. If material is not included in the article's Creative Commons license and your intended use is not permitted by statutory regulation or exceeds the permitted use, you will need to obtain permission directly from the copyright holder. To view a copy of this license, visit <http://creativecommons.org/licenses/by/4.0/>.

© The Author(s) 2022